An Event Set Mode Recognition Method for Fault Diagnosis of Inverter Output Overcurrent in Electric Traction System

Qiang Ni, *Member, IEEE*, Zhikai Chen, Aiyu Gu, Yang Meng, Jialin Li, Xueming Li, and Loi Lei Lai, *Life Fellow, IEEE*

***Abstract*—The inverter output overcurrent (IOO) is a common abnormal state in an electric traction system (ETS), which can be caused by several sources within the ETS and results in an immediate inverter shutdown and requires maintenance at the station. In order to improve the efficiency and intelligence level of maintenance, this article proposes an event set pattern identification method to trace the causes of IOO faults. First, according to traction motor control theory and overcurrent fault mechanism analysis, the several feature indicators of related system signals within the period of stator current are extracted by using adaptive sliding window technique. Second, based on historical data, an event generation method is investigated with hysteresis comparators by studying the variation laws of feature indicators, and event template sequence patterns are constructed to represent different fault causes. Then, the online diagnosis framework has been proposed, which includes three parts, namely, diagnostic enabling, event sampling sequence calculation and fault identification. Finally, field experiments are conducted, and the results show that the proposed method has excellent performance under changes in stator current frequency and operating conditions, and it also has a potential for practical applications.**

***Index Terms*—Electric traction system (ETS), event set pattern identification, fault diagnosis (FD), inverter output overcurrent (IOO), traction motor control.**

I. Introduction

ELECTRIC-TRACTION system (ETS) is a classical three-phase pulse-width modulation inverter fed induction motor drive system, which provides power for the train to move forward

Manuscript received 6 April 2024; revised 16 June 2024; accepted 11 August 2024. Date of publication 19 August 2024; date of current version 11 September 2024. This work was supported in part by the National Natural Science Foundation of China under Grant 62103109 and in part by the Natural Science Foundation of Guangdong Province under Grant 2024A1515011966. Recommended for publication by Associate Editor O. Trescases. *(Corresponding author: Aiyu Gu.)*

Qiang Ni, Zhikai Chen, Aiyu Gu, Yang Meng, and Jialin Li are with the Department of Electrical Engineering, School of Automation, Guangdong University of Technology, Guangzhou 510006, China (e-mail: nq666@gdut.edu.cn; 2112204493@mail2.gdut.edu.cn; guay@gdut.edu.cn; 2112204530@mail2.gdut.edu.cn; 2112204476@mail2.gdut.edu.cn).

Xueming Li is with the College of Mechanical and Vehicle Engineering, Hunan University, Changsha 410082, China (e-mail: lixm@hnu.edu.cn).

Loi Lei Lai was with the Guangdong University of Technology, Guangzhou 510006, China. He is now with the DRPT International Incorporated, Perth 6009, Australia (e-mail: l.l.lai@ieee.org).

Color versions of one or more figures in this article are available at https://doi.org/10.1109/TPEL.2024.3443288.

Digital Object Identifier 10.1109/TPEL.2024.3443288

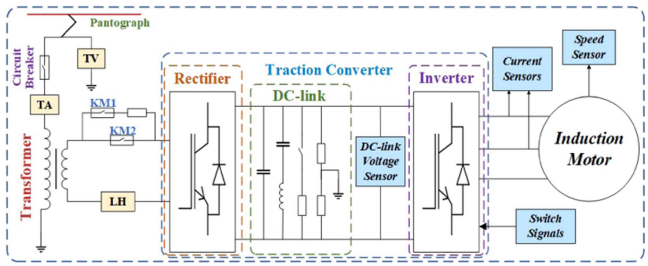

Fig. 1. Class ETDS circuit topology.

[1]. However, the ETS is prone to sudden electrical faults with the growth of the service time. Once occurred, if these faults are not detected and diagnosed in time, they may result in a reduction in the ETS's performance or even serious safety accidents [2]. Therefore, it is crucial to study effective fault diagnosis (FD) methods for ensuring safe and efficient train operation [3].

As shown in Fig. 1, the ETS consists of traction transformer module, rectifier module, traction inverter module, and traction motors. Previous studies of FD in ETS mainly focused on improving the diagnostic accuracy of a component or multiple components. For example, in the motor drive system, an open-circuit fault [4], a type of current sensor fault [5], interturn short circuit fault [6], and broken rotor bar fault [7] were reported. In [4], [5], [6], and [7], these research results only discussed the diagnosis of one type of component faults, ignoring the impact of other component failures. The inverter output current, motor speed, and intermediate dc voltage are the required sampling signals for closed-loop control of an induction motor drive system. However, the coupling relationship between these sensor signals is complex. Dong et al. [8] proposed a multisensor FD method. Due to the coupling relationship between sensor signals and insulated gate bipolar transistor (IGBT) pulse state signals, Gou et al. [4] proposed a data-driven based method for simultaneous diagnosis of IGBT and current sensor fault. A diagnosis method for IGBT, current, and speed sensor faults was proposed in [9]. However, ETS is a complex multimodule cascaded electromechanical coupling system, in which each module is closed-loop controlled and the energy transformation and transmission between modules have a complex relationship. Therefore, given the complexity of modules cascading and multi-closed-loop control, it is imperative that engineering and technical personnels need to explore functional FD and protection methods at the system

level. That is to ensure the safe and stable operation of trains, while studying how to improve the performance of component level FD.

In recent years, several system level FD results have been published. Chen et al. [10] diagnosed the cause of abnormal ground detection voltage of main circuit in the ETS by using canonical correlation analysis. Ni et al. [11] further improved its diagnostic performance through multi feature fusion technology. Ni et al. [12] studied the problem of grid side overcurrent fault in ETS and developed a Gaussian mixture model-hidden Markov model based diagnostic model to trace the cause of the fault. However, only a few research results have been published on the diagnosis of IOO issue.

Inverter output overcurrent (IOO) is a common system level fault in ETS. Once it occurs, the traction converter, including a rectifier and an inverter, will be blocked and the train will lose some power. The causes of IOO faults are diverse, and manual methods are still required to identify the cause of IOO faults. This not only leads to low maintenance efficiency, but also requires operators to have a good professional level. Therefore, there is an urgent need to study intelligent methods for tracing IOO faults to improve the intelligence level of train operation and protection. This article reports the research on the diagnosis of IOO faults.

The model-based FD method and data-based FD method are widely used in induction motor drive system [13]. The diagnostic performance of model-based methods is limited by the accuracy of the mechanism model [14]. For the IOO fault, the system structure before and after the fault will change due to the protection method of blocking the converter. Moreover, there are significant differences in the impact mechanisms of different fault causes. Therefore, the model-based FD method alone is not suitable for IOO FD since it is difficult to establish an accurate mathematical model. The data-driven methods diagnosed by mining potential patterns in data, and their performance do not depend on the accuracy of the mathematical models [15]. However, the IOO fault is a low probability event. Moreover, the time from fault occurrence to protection is relatively short. It is difficult to collect a large number of data samples. Therefore, this article will synthesize the data and model based on interest and experience.

Generally, dc-link voltage, traction motor speed and output current in traction inverter system are continuously changed and have obvious temporal characteristics. Chen et al. [10] and Ni et al. [11] [12] have made good progress in system level FD by mining the time series patterns of correlated signals. Compared with the main circuit grounding fault [10], [11], the impact of IOO fault on the system is more severe. The grounding detection voltage is only for monitoring the status, while the output current of the inverter needs to participate in closed-loop control. After the grounding detection signal is abnormal, the system's operating status will not change and can last for a long time. However, once the inverter experiences an overcurrent, the system will take measures to block the pulse for protection, within a short duration. In grid side overcurrent faults [12], the grid current is with a fixed power frequency of 50 Hz, while in IOO faults, the stator current frequency of the traction motor is variable and not constant at 50 Hz. Therefore, it remains a challenging issue to use the time series characteristics of signals for IOO FD.

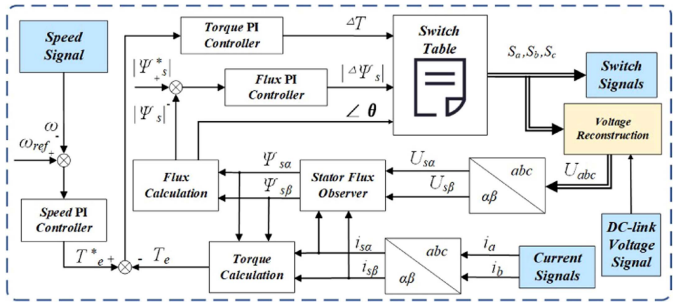

Fig. 2. Schematic diagram of DTC circuit for inverter drive.

Motivated by the aforementioned research gap, this study proposes the diagnosis method for IOO fault, which combines the characteristics of data and knowledge. The main contributions of this article are summarized as follows.

1) The IOO fault mechanism is analyzed by studying the time series variation laws of sample signals in traction motor control system. A feature index extraction method combining fast Fourier transform (FFT) and adaptive sliding window is proposed, which fully considers the characteristics of motor stator current frequency variation.
2) The variation laws of characteristic indicators for fault causes are investigated and the event generation methods are proposed by using hysteresis technology. The event template sequence patterns are constructed to represent the different fault causes.
3) An FD framework for event set identification is proposed by incorporating diagnostic enabling, event sampling sequence calculation, and fault identification. The effectiveness of the approach is validated based on on-site fault scenario reconstruction and digital signal processing (DSP) controller execution of diagnostic programs.

The rest of this article is organized as follows. Section II briefly introduces the control strategy of ETS and the mechanism of traction motor overcurrent fault. In Section III-A, the adaptive sliding window model, eigenvalue acquisition, and generation of operational condition events are proposed. In Section III-B, a diagnostic framework based on event sequence pattern identification is proposed to trace the causes of faults. Section IV validates the effectiveness of the diagnostic model through comparative experiments. Finally, Section V concludes this article.

II. Mechanism Analysis of IOO Faults

A. Principle of Inverter Drive Circuit

As shown in Fig. 1, the ETS consists of traction transformer, four quadrant pulse rectifier, traction inverter, and traction motors, which takes a single-phase alternating current (ac) of 25 kV from the power grid through a pantograph and converts it to power the variable frequency three-phase ac drive traction motors [16]. After the system startup is completed, the operating conditions of the traction inverter can be defined as two types, that is, blocked pulse (W_1) and normal operation (W_2) [17].

TABLE I
SOURCES OF INVERTER OUTPUT OVERCURRENT FAULTS

Number	Fault code	Fault cause
1	C_1	Speed sensor signal fault
2	C_2	Traction Motor Fault
3	C_3	DC-link Voltage Sensor Fault
4	C_4	Inverter IGBT Module Fault

In order to achieve superior dynamic and static performance, the direct torque control (DTC) [18] strategy is a classical solution for traction motor control, which is performed in the traction control unit (TCU). As shown in Fig. 2, TCU samples the signals including dc-link voltage, stator currents, and motor speed to achieve closed-loop control. DTC is also essentially for stator current decoupling control. Therefore, in this article, the time series variation laws of these signals within the stator current cycle will be explored to investigate the causes of IOO.

B. Analysis of Overcurrent Type

Once the output current exceeds a predefined threshold, the system triggers an alarm, this represents an "IOO" The TCU will then block the pulsewidth modulation pulses, and the inverter will shut down, the operating conditions of ETS will be switched from W_2 to W_1. Based on historical maintenance experience, the main causes of IOO faults include speed sensor signal fault, traction motor fault, dc-link voltage sensor fault and inverter IGBT module fault, as given in Table I.

1) Speed Sensor Signal Fault: The speed closed-loop is crucial for improving the fast response of operating conditions changes, such as uphill and downhill, acceleration and deceleration. The velocity of a train's bogie is determined by multiple traction motors working in unison. When a speed measurement circuit experiences sudden variations, for example, signal loss, or interference, the proportion integral controller quickly reaches saturation, causing the motor to produce maximum acceleration or deceleration torque. Then, the IOO fault will occur owing to the speed difference with other traction motors, which may cause the motor to stall or drag. As shown in Fig. 3(a), for a speed sensor signal fault, the A-phase current I_a exhibits with a gradual divergence of double shoulders under the W_2, and its amplitude is significantly larger than that of B-phase current I_b. Meanwhile, the absolute value the current amplitude increases gradually in half a period. When switching from W_2 to W_1, the speed measurement signal will change suddenly. In fact, the motor speed will not change suddenly, since the train has a large moment of inertia

2) Traction Motor Fault: For traction motors, when operating in demanding and harsh environmental conditions, are prone to various faults, such as stator inter-turn short circuits, rotor malfunctions, and bearing failures [19]. Among these faults, stator inter-turn short circuit is the most common fault, which can lead to IOO phenomenon based on extensive on-site maintenance experience. When a stator inter-turn short circuit occurs, it induces harmonic current components that cyclically propagate between the stator and rotor windings, as manifested

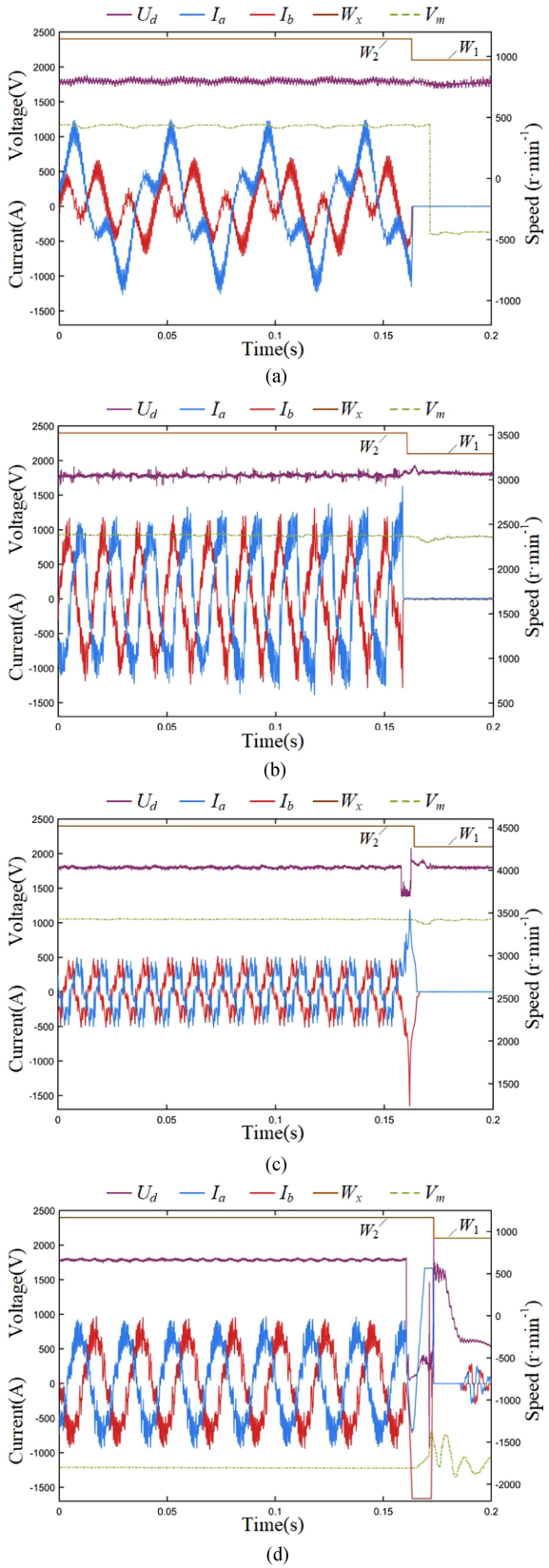

Fig. 3. (a) Speed sensor signal fault. (b) Traction motor fault. (c) DC-link voltage measuring circuit fault. (d) Traction converter module fault.

by (1). The escalation of higher-order harmonic components contributes to the emergence of overcurrent phenomena in the inverter output [20]

$$f_s = [a \pm b(1-s)/p]f \tag{1}$$

where f is the stator current fundamental frequency, s is the slip rate and p is the number of pole pairs, a = 1,3 b = 1, 2, 3, …, (2p-1).

As shown in Fig. 3(b), when a traction motor fault caused by stator inter-turn short circuit, the stator currents do not exhibit distortion, but show a divergent trend, and the absolute values of current amplitude gradually increase within half a cycle. The dc-link voltage signal exhibits pronounced spike disturbances under W_2. When the operating conditions transitioning to W_1, the spike disturbances in the dc-link voltage signal disappear. In contrast to the speed sensor fault, the speed signal remains unchanged under this fault condition.

3) DC-Link Voltage Measuring Circuit Fault: The dc-link voltage signal and the switching signals are subject to voltage reconstruction. By following (2), this results in the generation of three-phase voltages. Both the voltage and sampled current information are used as inputs of flux observer and calculate the motor stator flux, achieving the closed-loop control

$$\begin{bmatrix} U_a \\ U_b \\ U_c \end{bmatrix} = U_d \begin{bmatrix} 2/3 & -1/3 & -1/3 \\ -1/3 & 2/3 & -1/3 \\ -1/3 & -1/3 & 2/3 \end{bmatrix} \begin{bmatrix} S_a \\ S_b \\ S_c \end{bmatrix}. \tag{2}$$

In the case of a fault in the dc-link voltage signal, there may be significant deviations in the torque and magnetic flux calculations. As shown in Fig. 3(c), an abrupt decline in the dc-link voltage is observed under W_2. Accompanied by rapid divergence of currents, this surpasses the protection threshold. Upon transitioning to W_1, the dc-link voltage is restored to its initial state. The speed signal remains unaffected by the dc-link sensor fault.

4) Traction Converter Module Fault: The traction converter achieves energy conversion by controlling IGBTs turn ON or OFF. With the increase of service time, IGBTs are prone to open circuit or short-circuit faults, leading to sudden fluctuations in dc-link voltage and the occurrence of IOO faults. As shown in Fig. 3(d), for a traction converter module fault, a sudden inverter fault occurs, causing the dc-link voltage signal to instantaneously drop to near-zero levels under W_2. Concurrently, currents rapidly diverge, surpassing the protection threshold, and the speed signal exhibits fluctuations. Upon receiving a blocking signal and transitioning to W_1, the dc-link voltage signal gradually restores to its normal level before quickly decreasing once again.

Based on the above analysis, different causes of IOO faults have fault characteristics in terms of dc-link voltage, three-phase currents, motor speed and operation conditions. Therefore, in this article, these signals are selected and their temporal variation laws are deeply extracted to diagnose the causes of the IOO fault.

III. Proposed Diagnosis Method for IOO Fault

In this section, our idea is introduced, which mainly includes extracting the characteristic indicators of the correlated signals within the stator current cycle, analyzing the time series change laws of the characteristic indicators, generating discrete event sequences, characterizing each fault source with event sequence patterns, and identifying fault patterns.

A. Event Set Characterization of Each Fault Cause

1) Adaptive Frequency Sliding Window: According to electric machine theory, the relationship between induction motor speed V_m, stator current frequency f, and pole pairs number p can be expressed as

$$V_m = \frac{60f}{p}. \tag{3}$$

Since the traction train is a large inertial system, the IOO takes a very short time from occurrence to diagnosis, and the true speed of the train can be regarded as unchanged during this time. Therefore, the article adopts the mode of adjustment sliding window based on traction motor current frequency for feature index calculation. Initially, distinct current frequencies are extracted with (4) and (5) as shown below. More FFT details can be found in [21]

$$X(k) = \sum_{n=0}^{N-1} x(n) e^{-\frac{j2\pi nk}{N}}, k = 0, 1, 2, \ldots, N-1 \tag{4}$$

$$f_I = \text{IDFT}\left(\max X(k) e^{\frac{j2\pi nk}{N}}\right) T_s \tag{5}$$

where N is the number of current data samples, k is the system operation time, f_I is the frequency of current and T_s is the data sampling period.

Subsequently, by employing (6) and (7), the window size and step size corresponding to the extracted frequency are precisely determined

$$K_N = \left(\frac{1}{f_I T_s}\right) \tag{6}$$

$$S_{\text{step}} = K_N/2 \tag{7}$$

where K_N is the number of sliding window data and S_{step} is the sliding window step size.

After this the required feature metrics within a designated sliding window can then be calculated.

2) Feature Indicators Extraction and Analysis: In order to better explore the time series characteristics of the correlation signals within the stator current cycle, the time-domain characteristic indicators are extracted by (8) to (15), which include the minimum value of the dc-link voltage (J_1), the variance of the dc-link voltage (J_2), the variance of the motor speed (J_3), and the root mean square value of the normalized phase currents (J_5). Furthermore, the absolute value of the time-domain statistical measures of the normalized currents (J_4) is utilized to depict the changes in fault characteristic variables throughout the entire data

$$Q_x(k) = \frac{1}{K_N} \sum_{i=1}^{K_N} x(k-i+1), x \in (U_d, V_m) \tag{8}$$

$$I_{x\min}(k) = \min[I_x(k), I_x(k-1), \ldots, I_x(k-N+1)] \tag{9}$$

TABLE II
CHANGE RULES OF INDICATOR CHARACTERISTICS

Feature Indicator	Operation Condition	Change Rule Description			
		C_1	C_2	C_3	C_4
J_1	W_2	$\geq T_{1on}$	$\geq T_{1on}$	$\geq T_{1on}$	$\geq T_{1on}$
	$W_2 \rightarrow W_1$			$\leq T_{1off}$	$\leq T_{1off}$
J_2	W_2	$\leq T_{2off}$	$\leq T_{2off}$	$\leq T_{2off}$	$\leq T_{2off}$
	$W_2 \rightarrow W_1$			$T_{2off} < J_2 < T_{2on}$	$\geq T_{2on}$
J_3	W_2	$\leq T_{3off}$	$\leq T_{3off}$	$\leq T_{3off}$	$\leq T_{3off}$
	$W_2 \rightarrow W_1$	$\geq T_{3on}$			$T_{3off} < J_3 < T_{3on}$
J_4	W_2	$\leq T_{4off}$	$\leq T_{4off}$	$\leq T_{4off}$	$\leq T_{4off}$
	$W_2 \rightarrow W_1$	$\geq T_{4on}$	$\geq T_{4on}$	$\geq T_{4on}$	$\geq T_{4on}$
J_5	W_2	$\geq T_{5on}$	$\geq T_{5on}$	$\geq T_{5on}$	$\geq T_{5on}$
	$W_2 \rightarrow W_1$	$\leq T_{5off}$	$\leq T_{5off}$	$\leq T_{5off}$	$\leq T_{5off}$

$$I_{x\max}(k) = \max[I_x(k), I_x(k-1), \ldots, I_x(k-N+1)] \tag{10}$$

$$J_1(k) = \min[U_d(k), U_d(k-1), \ldots, U_d(k-K_N+1)] \tag{11}$$

$$J_2(k) = \frac{1}{K_N - 1} \sum_{i=1}^{K_N} [U_d(k-i+1) - Q_{U_d}(k)]^2 \tag{12}$$

$$J_3(k) = \frac{1}{K_N - 1} \sum_{i=1}^{K_N} [V_m(k-i+1) - Q_{V_m}(k)]^2 \tag{13}$$

$$J_4(k) = \left| \frac{I_x(k) - I_{x\min}(k)}{I_{x\max}(k) - I_{x\min}(k)} \right| \tag{14}$$

$$J_5(k) = \sqrt{\frac{1}{K_N} \int_0^{K_N} {I_x}^2(t) dt} \tag{15}$$

where N is the length of extracted data, $I_x \in (I_a, I_b)$.

According to the study of historical data samples, it was found that the characteristic indicators ($J_1 \sim J_5$) exhibit a variation law from IOO fault occurrence to protection, as given in Table II.

3) Event Sequence Generation: The relationship between feature indicators and hysteresis comparator thresholds are defined as events. In this article, five feature indicators can be extracted by (16), corresponding to this, five hysteresis comparators will be set, and five events will be defined. The threshold values in Table II for event triggering are empirically set. The event state at time k can be described as

$$E_x(k) = \begin{cases} 1, & J_x \geq T_{x\text{on}} \\ E_x(k-1), & T_{x\text{off}} < J_x < T_{x\text{on}} \\ 0, & J_x \leq T_{x\text{off}} \end{cases} \quad x \in (1,2,3,4,5) \tag{16}$$

where $T_{x\text{on}}$ and $T_{x\text{off}}$ represent the upper and lower threshold values of the xth hysteresis comparator, respectively. If the value of the feature indicator is greater than the upper limit threshold of the corresponding hysteresis comparator, the corresponding event will be set to 1. On the contrary, if the value is less than the lower limit threshold of the corresponding hysteresis comparator, the event will be set to 0. If the value is between the upper limit threshold and the lower limit threshold, the event will remain unchanged. For example, at time k, if the $J_1(k) \geq T_{1\text{on}}$, then $E_1(k)$ is set to 1, if the $J_1(k) \leq T_{1\text{off}}$, then the $E_1(k)$ is set to 0. if $J_1(k) \in (T_{1\text{off}}, T_{1\text{on}},)$, the $E_1(k)$ is equal to $E_1(k\text{-}1)$.

When the IOO occurs, the operating condition of traction inverter changes from normal (W_2) to pulse blocking condition (W_1). The E_5 can be defined to describe the switching of these states, as follows:

$$W_x(k) = \begin{cases} W_2(k), & E_5(k) = 1 \\ W_1(k), & E_5(k) = 0 \end{cases}. \tag{17}$$

4) Event Set Template for Fault Causes: The output current of the inverter varies continuously from normal to abnormal, and then to protection, with the associated signals exhibiting a certain temporal variation pattern. Based on the field data case, the event triggering law is analyzed, and the event template sets for each IOO fault type are defined as given in Table III. Each sample includes the start flag, diagnostic set and end flag. Defining the diagnostic universal set as

$$D_U\,|W_2 = \{\, E_i = 1 |\, i = (1,2,3,4,5)\}\,. \tag{18}$$

Taking the case of a speed sensor signal fault (C_1) case as an example, the system enters the diagnostic mode when the start flag ($S = 1$ under W_2) is set to 1 and the diagnosis ends, when the end flag ($E_{\text{end}} = 1$ under W_1) is set to 1. From the beginning to the end of diagnosis, the collected event set contains the diagnostic set D_{C1}, it means that the fault type is C_1.

TABLE III
TEMPLATE LIBRARY OF EVENT SETS FOR EACH IOO FAULT TYPE

Fault code	Start Flag	Diagnostic Set	End Flag
C_1	W_2: S=1	W_2: D_{C1}= {E_i=1|i= (1,3,4,5)}	W_1: E_{end}=1
C_2	W_2: S=1	W_2: D_{C2}= {E_i=1|i= (1,4,5)}	W_1: E_{end}=1
C_3	W_2: S=1	W_2: D_{C3}= {E_i=1|i= (4,5)}	W_1: E_{end}=1
C_4	W_2: S=1	W_2: D_{C4}= {E_i=1|i= (2,4,5)}	W_1: E_{end}=1

B. Diagnostic Framework

1) Diagnostic Enable: In order to reduce the computational complexity of diagnostic units, the proposed fault detection approach uses S as fault diagnostic enable index. When the sampled inverter output current continuously exceeds the threshold value (I_{Th}) five times, the S will be set to 1 and the classification and isolation process is enabled. It is expressed as

$$S\,|W_2 = \begin{cases} 1, & |I_x| \geq |I_{Th}| \text{ and } m > 5 \\ 0, & \text{others} \end{cases} \tag{19}$$

where the variable m represents the number of consecutive times the threshold value (I_{Th}) has been exceeded.

2) Time Series Event Set Calculation: When the diagnosis module is enabled, the diagnosis unit reads the data from the data buffer. The time series feature indexes are calculated from (8) to (15) and time series event sequence is generated from (16). In this article, a total of five events have been defined. Assuming

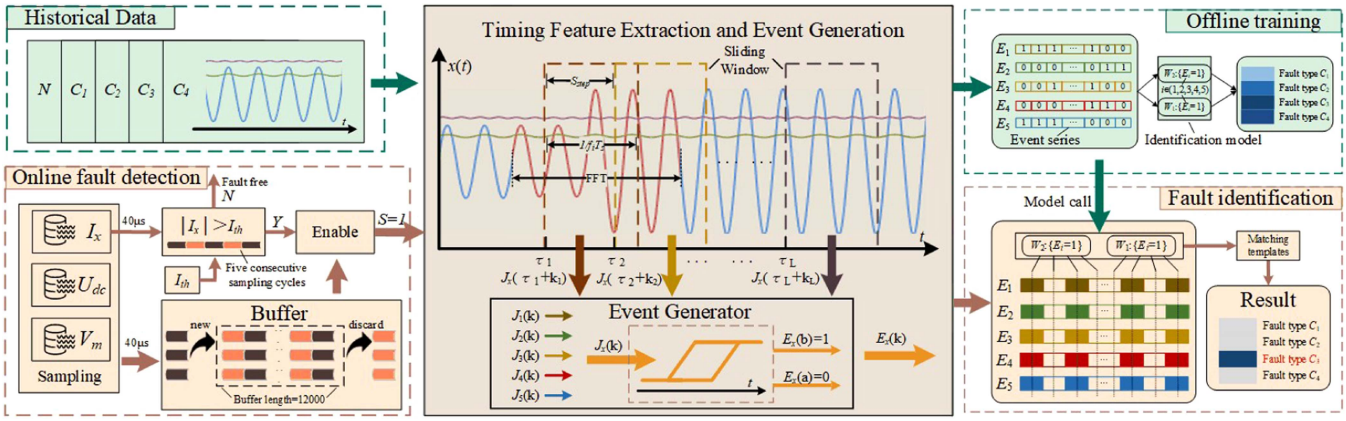

Fig. 4. Diagnostic flowchart.

at time k, the event state vector can be defined as

$$\overrightarrow{O_k} = [E_1, E_2, E_3, E_4, E_5]^T. \tag{20}$$

The generated vector $\overrightarrow{O_k}$ is collected continuously until the end flag $E_{\text{end}} \,|\, W_1 = 1$, with a total of L observation vectors. It can be defined as

$$O = \left[\overrightarrow{O}_1 \to \overrightarrow{O}_2 \to \cdots \to \overrightarrow{O}_L\right] = \begin{bmatrix} E_{11} & \to & E_{12} & \to \cdots \to & E_{1L} \\ E_{21} & \to & E_{22} & \to \cdots \to & E_{2L} \\ E_{31} & \to & E_{32} & \to \cdots \to & E_{3L} \\ E_{41} & \to & E_{42} & \to \cdots \to & E_{4L} \\ E_{51} & \to & E_{52} & \to \cdots \to & E_{5L} \end{bmatrix} \tag{21}$$

$$E_{\text{end}} \,|\, W_1 = \begin{cases} 1, & \overrightarrow{O_k} = [1,0,0,0,0]^T \\ 0, & \text{others} \end{cases} \tag{22}$$

where $L = N{\cdot}T_{\text{s}}$ and "$\to$" denotes the moment of transition.

Then, the event diagnostic set is constructed based on the obtained O, defined as

$$D\,|W_2 = \{E_{11}, \cdots, E_{1k}, E_{21}, \cdots, E_{2k}, \cdots, E_{51}, \cdots, E_{5k}\}. \tag{23}$$

3) Fault Identification: Due to the slow changing process of the inverter output current from abnormal to overcurrent and then to protection, the sampled event diagnosis set D contains several identical events. Therefore, on the basis of studying the changing patterns of events in historical fault samples, each event sequence can be represented by an event state. It can be defined as

$$E_i \,|\, W_2 = \begin{cases} E_{i1} \wedge E_{i2} \wedge, \ldots, \wedge E_{ik} & i \in (1,5) \\ E_{i1} \vee E_{i2} \vee, \ldots, \vee E_{ik} & i \in (2,3,4) \end{cases} \tag{24}$$

$$W_2 : D = \{E_1\,|W_2\,, E_2\,|W_2\,, E_3\,|W_2\,, E_4\,|W_2\,, E_5\,|W_2\} \tag{25}$$

$$W_2 : D \cap D_U = C. \tag{26}$$

With this, the intersection C is extracted, which will be matched with the diagnostic template set D_{Cx} and the result will be used to determine the fault type C_x

$$W_2 : C = D_{C_x} \quad \Rightarrow \quad C_x \quad . \tag{27}$$

For example, by identifying a speed signal fault, this can give the identification result in

$$W_2 : C = \{E_i = 1 | \, i = (1,3,4,5)\} = D_{C_1} \quad \Rightarrow \quad C_1 \quad . \tag{28}$$

To sum up, the block diagram of the proposed diagnosis method is shown in Fig. 4, which can be divided into offline part and online part. In the offline part, the pattern of feature extraction and event generation is established for feature extraction and event generation, and the diagnostic template sets are constructed based on historical data. And in the online part, the fault detection module detects two phase currents in real-time and determines whether it is an overcurrent. When the IOO occurs, the detection module will enable the diagnosis module, then, the signals of dc-link voltage, two phase currents and speed will read from data buffer, which are used for calculating the sliding window size and feature indicators. The event set is generated and simplified for matching the template and obtaining the diagnosis results.

IV. Field Data Validation

A. Data Description

To verify the effectiveness of the proposed diagnosis method, the experiment based on on-site fault recording data is carried out, as shown in Fig. 5 . When a train experiences an IOO fault during operation, the TCU will record a segment of data before and after the fault as field case data, including dc-link voltage signals, A and B-phase current signals and speed sensor signals. In this article, we collected a total of 46 cases, including four types of faults, this includes 8000 points before the inverter pulse blocking and 4000 points after the pulse blocking. In order to reproduce the fault scenario, the fault case data of waveform recording is played in a loop by RT-LAB, and then, the diagnostic algorithm is implemented in a DSP, which produces enough information including dc-link voltage signals, A and B-phase current signals and speed sensor signals with a period of 40 μs,

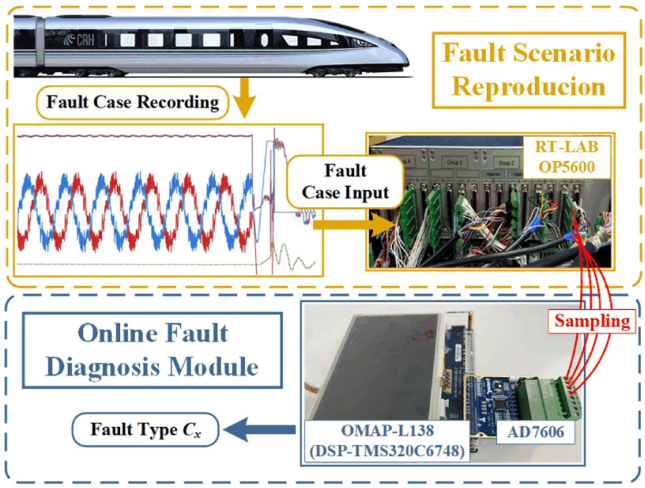

Fig. 5. Fault scenario reproduction online diagnostics.

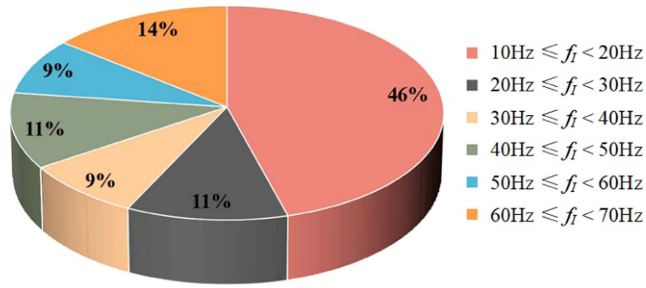

Fig. 6. Percentage of different frequency in total fault samples.

and stores the latest 2000 collected points into the buffer store through the direct memory access channel.

The DSP determines in real-time whether there is an overcurrent fault. Once it is detected, it reads data from buffer and executes the fault identification.

To demonstrate the superiority of the diagnosis method proposed in this article, four diagnosis methods were introduced for comparison. The methods are the fixed sliding window and nonhysteresis comparators (FSW-NHC), fixed sliding window and hysteresis comparators (FSW-HC), adaptive frequency sliding window and nonhysteresis comparators (AFSW-NHC) and adaptive frequency sliding window and hysteresis comparators (AFSW-HC).

B. Performance Indicator

To evaluate diagnostic performance, the average time of FD (T_{ad}), i.e., from the time the DSP detects the occurrence of IOO to the end of the diagnosis, and the correct identification rate (CIR) are used to compare the performance of proposed model as shown in [12], and the calculation of CIR can be given as follows:

$$P_{\mathrm{CIR}} = \frac{\mathrm{Num}(C_{\mathrm{judge}} = C_i | C_{\mathrm{real}} = C_i)}{N_f} \times 100\% \tag{29}$$

where N_f is the total number of IOO cases, C_{judge} is diagnosis result of the model, and C_{real} is the real IOO type of each case.

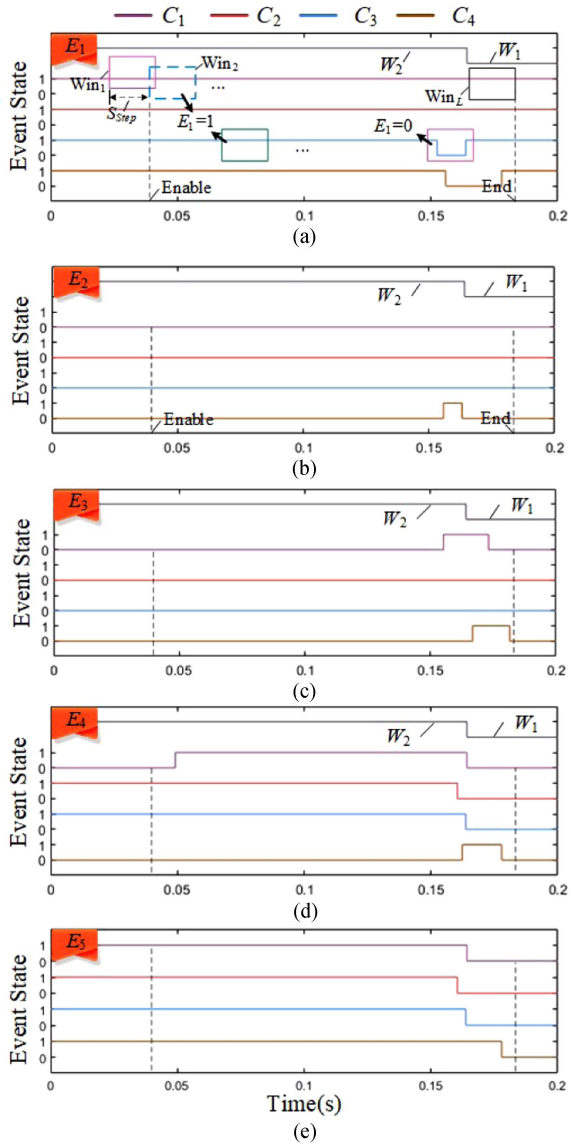

Fig. 7. The changing patterns of events for four fault types. (a) E_1. (b) E_2. (c) E_3. (d) E_4. (e) E_5.

TABLE IV
CIR RESULT OF DIFFERENT MODELS

Model	Fault Type				
	C_1	C_2	C_3	C_4	T_{ad}
FSW-NHC	41.60%	33%	51.2%	33.30%	0.221s
FSW-HC	55.40%	100%	66.60%	66.60%	0.221s
AFSW-NHC	62.50%	66.60%	76.60%	100%	0.194s
AFSW-HC	91%	100%	100%	100%	0.194s

C. Results Analysis

The proposed method (AFSW-HC) is compared against FSW-NHC, FSW-HC, and ASFW-NHC methods. As given in Table IV, both the hysteresis comparator and the adaptive frequency sliding window can significantly improve diagnostic

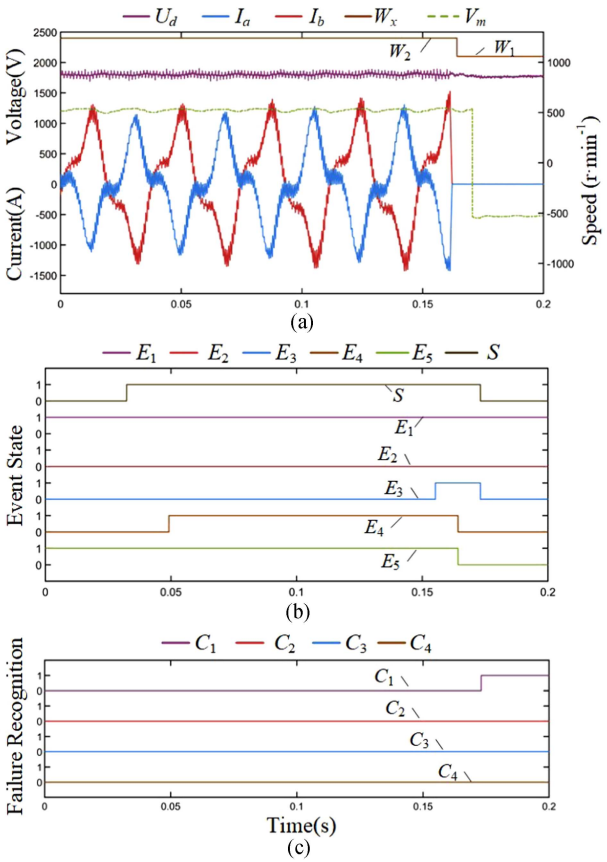

Fig. 8. Diagnosis results for C_1 case. (a) Sampling data. (b) Changes in event status. (c) Fault identification results.

performance among the four fault types. The CIR value of FSW-HC is 13.8% higher than FSW-NHC for the case of C_1. This is because the operating conditions of trains change in real-time, such as uphill, downhill, light and heavy loads, and then, there is a certain fluctuation range of characteristic indicators. The CIR value of AFSW-HC is 7.1% higher than FSW-HC for the case of C_1. As shown in Fig. 6, when an overcurrent fault occurs, the frequency of the output current from the inverter is random, and the determination of the sliding window size depends on the current period. Because of this, the T_{ad} of the diagnosis method using the AFSW is shorter than that of FSW, and AFSW takes less time to calculate the characteristic indicator diagnosis when diagnosing faults with large current period. Fewer diagnostic times can help on-board systems to quickly isolate faulty components and prevent faults from spreading. The results in Table IV show that the proposed AFSW-HC method has an obvious superior performance.

Fig. 7 shows the changing patterns of events ($E_1 \sim E_5$) from enabling diagnosis to ending diagnosis. Each sliding window will generate an event. During the process, event sequence will be obtained, and the theoretical reasoning will be obtained with (21), (22), (23). As shown in Fig. 6(a), event sequence E_1 has the same state for many times, which means that many repeated events are in the event sequence. Therefore, according to (26), event sequence simplification should be performed.

Fig. 8 shows the diagnosis results for case C_1 by the proposed method. As shown in Fig. 8(a), the overcurrent occurs at the peak of phase A current around 0.02 s and the overcurrent occurs again at the trough position. Then, the FD module is enabled, and S is set to 1. As shown in Fig. 8(b), E_1, E_3, and E_4 have 1 state. Therefore, after the event sequence is simplified, the fault type can be diagnosed as C_1 shown in Fig. 8(c).

V. Conclusion

The manual troubleshooting is the existing method of tracing the cause of IOO faults in ETS, which has problems of low maintenance efficiency and low level of train intelligence. To solve this issue, this article proposed a real-time diagnosis method for IOO faults by mining the temporal variation pattern of correlation signal feature indicators within the stator current cycle. A feature extraction method based on adaptive sliding window and FFT technology is proposed to address the characteristics of stator current changes. The event sequence can be generated by the variation laws of the feature indicator and the characteristics of each the fault cause can be represented by event sets. Then, the IOO fault tracking problem is transformed into a time set recognition problem. Finally, based on the recorded data from the fault site, the fault scenario was reproduced, and the diagnostic program was executed in DSP. The effectiveness of the proposed method was verified through comparative experiments. The proposed method has the characteristics of simple structure and low computational complexity, and has good engineering prospects, which is helpful to improve the intelligence of train state perception and maintenance. Our future work will further study its on-board diagnostic system.

References

[1] X. Li, J. Xu, Z. Chen, S. Xu, and K. Liu, "Real-time fault diagnosis of pulse rectifier in traction system based on structural model," *IEEE Trans. Intell. Transp. Syst.*, vol. 23, no. 3, pp. 2130–2143, Mar. 2022.

[2] K. Zhang, B. Gou, W. Xiong, and X. Feng, "An online diagnosis method for sensor intermittent fault based on data-driven model," *IEEE Trans. Power Electron.*, vol. 38, no. 3, pp. 2861–2865, Mar. 2023.

[3] H. Chen and B. Jiang, "A review of fault detection and diagnosis for the traction system in high-speed trains," *IEEE Trans. Intell. Transp. Syst.*, vol. 21, no. 2, pp. 450–465, Feb. 2020.

[4] B. Gou, Y. Xu, Y. Xia, Q. Deng, and X. Ge, "An online data-driven method for simultaneous diagnosis of IGBT and current sensor fault of three-phase PWM inverter in induction motor drives," *IEEE Trans. Power Electron.*, vol. 35, no. 12, pp. 13281–13294, Dec. 2020, doi: 10.1109/TPEL.2020.2994351.

[5] Y. Yu, Y. Zhao, B. Wang, X. Huang, and D. Xu, "Current sensor fault diagnosis and tolerant control for VSI-based induction motor drives," *IEEE Trans. Power Electron.*, vol. 33, no. 5, pp. 4238–4248, May 2018.

[6] V. Gurusamy, E. Bostanci, C. Li, Y. Qi, and B. Akin, "A stray magnetic flux-based robust diagnosis method for detection and location of interturn short circuit fault in PMSM," *IEEE Trans. Instrum. Meas.*, vol. 70, 2021, Art. no. 3500811.

[7] W. Wang, X. Song, G. Liu, Q. Chen, W. Zhao, and H. Zhu, "Induction motor broken rotor bar fault diagnosis based on third-order energy operator demodulated current signal," *IEEE Trans. Energy Convers.*, vol. 37, no. 2, pp. 1052–1059, Jun. 2022.

[8] H. Dong, F. Chen, Z. Wang, L. Jia, Y. Qin, and J. Man, "An adaptive multi-sensor fault diagnosis method for high-speed train traction converters," *IEEE Trans. Power Electron.*, vol. 36, no. 6, pp. 6288–6302, Jun. 2021.

[9] I. Jlassi and A. J. M. Cardoso, "A single method for multiple IGBT, current, and speed sensor faults diagnosis in regenerative PMSM drives," *IEEE J. Emerg. Sel. Top. Power Electron.*, vol. 8, no. 3, pp. 2583–2599, Sep. 2020.

[10] Z. Chen, X. Li, C. Yang, and T. Peng, "A data-driven ground fault detection and isolation method for main circuit in railway electrical traction system," *Instrum. Soc. America Trans.*, vol. 87, pp. 264–271, Apr. 2019.
[11] Q. Ni, X. Li, Z. Chen, Z. Zhao, and L. L. Lai, "A mechanism and data hybrid-driven method for main circuit ground fault diagnosis in electrical traction system," *IEEE Trans. Ind. Electron.*, vol. 70, no. 12, pp. 12806–12815, Dec. 2023.
[12] Q. Ni, Z. Zhan, X. Li, Z. Zhao, and L. L. Lai, "A real-time fault diagnosis method for grid-side overcurrent in train traction system using signal time series feature pattern recognition," *IEEE Trans. Ind. Electron.*, vol. 71, no. 4, pp. 4210–4218, Apr. 2024, doi: 10.1109/TIE.2023.3273260.
[13] H. Chen, B. Jiang, S. X. Ding, and B. Huang, "Data-driven fault diagnosis for traction systems in high-speed trains: A survey, challenges, and perspectives," *IEEE Trans. Intell. Transp. Syst.*, vol. 23, no. 3, pp. 1700–1716, Mar. 2022.
[14] Z. Gao, C. Cecati, and S. X. Ding, "A survey of fault diagnosis and fault-tolerant techniques—Part I: Fault diagnosis with model-based and signal-based approaches," *IEEE Trans. Ind. Electron.*, vol. 62, no. 6, pp. 3757–3767, Jun. 2015.
[15] Z. Chen et al., "A data-driven ground fault detection and isolation method for main circuit in railway electrical traction system," *Instrum. Soc. America Trans.*, vol. 87, pp. 264–271, Apr. 2019.
[16] Z. Liu, C. Xiang, Y. Wang, Y. Liao, and G. Zhang, "A model-based predictive direct power control for traction line-side converter in high-speed railway," *IEEE Trans. Ind. Appl.*, vol. 53, no. 5, pp. 4934–4943, Sep./Oct. 2017, doi: 10.1109/TIA.2017.2714624.
[17] H. Tao, T. Peng, C. Yang, S. Yin, Z. Chen, and X. Fan, "A diagnosis method for IGBT and current sensor faults of two-level inverter used in traction systems," in *Proc. CAA Symp. Fault Detection, Supervision, Saf. Tech. Processes*, 2021, pp. 1–6.
[18] W. Xu, M. M. Ali, M. F. Elmorshedy, S. M. Allam, and C. Mu, "One improved sliding mode DTC for linear induction machines based on linear metro," *IEEE Trans. Power Electron.*, vol. 36, no. 4, pp. 4560–4571, Apr. 2021, doi: 10.1109/TPEL.2020.3025184.
[19] T. Peng, C. Ye, and Z. Chen, "Stacking model-based method for traction motor fault diagnosis," in *Proc. CAA Symp. Fault Detection, Supervision Saf. Tech. Processes*, 2019, pp. 850–855,.
[20] J. Penman, H. G. Sedding, B. A. Lloyd, and W. T. Fink, "Detection and location of interturn short circuits in the stator windings of operating motors," *IEEE Trans. Energy Convers.*, vol. 9, no. 4, pp. 652–658, Dec. 1994, doi: 10.1109/60.368345.
[21] H. Kanders, T. Mellqvist, M. Garrido, K. Palmkvist, and O. Gustafsson, "A 1 million-point FFT on a single FPGA," *IEEE Trans. Circuits Syst. I, Reg. Papers*, vol. 66, no. 10, pp. 3863–3873, Oct. 2019, doi: 10.1109/TCSI.2019.2918403.

Qiang Ni (Member, IEEE) received the M.S. and Ph.D. degrees in electrical engineering from Southwest Jiaotong University, Chengdu, China, in 2013 and 2018, respectively.

He is currently a Lecturer with the Guangdong University of Technology, Guangzhou, China. His research interests include the intelligent fault diagnosis and health management for the power drive system, and intelligent control system for multienergy system.

Zhikai Chen received the B.E. degree in electrical engineering and automation in 2022 from the Guangdong University of Technology, Guangzhou, China, where he is currently working toward the master's degree in electrical engineering with the School of Automation, Guangdong University of Technology, Guangzhou, China.

His current research interests include fault diagnosis of traction drive systems.

Aiyu Gu received the B.S., M.S., and Ph.D. degrees in electrical engineering from the Harbin Institute of Technology, Harbin, China, in 1992, 1995, and 1998, respectively.

She is currently an Associate Professor with the School of automation, Guangdong University of Technology, Guangzhou, China. Her research interests include electric machines and control, and fault diagnosis, and unconventional electromagnetic device.

Yang Meng received the B.E. degree in automation from the Tianjin Chengjian University, Tianjin, China, in 2018. He is currently working toward the master's degree in electrical engineering with the School of Automation, Guangdong University of Technology, Guangzhou, China.

His current research interests include fault diagnosis of traction drive systems.

Jialin Li received the B.E. degree in electrical engineering and automation from the Beijing Normal University, Zhuhai, China, in 2022. He is currently working toward the master's degree in electrical engineering with the School of Automation, Guangdong University of Technology, Guangzhou, China.

His current research interests include fault diagnosis of traction drive systems.

Xueming Li received the bachelor's degree in automation from the Hunan Institute of Engineering and the master's degree in control science and engineering from Central South University, Changsha, China, in 2008 and 2011, respectively.

He is currently a Senior Engineer with Zhuzhou CRRC Times Electric Company, Ltd., Zhuzhou, China. His research interests include control, fault diagnosis, and prediction of rail vehicle traction electric drive systems.

Loi Lei Lai (Life Fellow, IEEE) received the B.Sc. (first-class Hons.) and Ph.D. degrees in electrical and electronic engineering from the University of Aston, Birmingham, U.K., in 1980 and 1984, respectively, and the D.Sc. degree in electrical and electronic engineering from the City University of London, London, U.K., in 2005.

He is currently the Chair of DRPT International Incorporated, Perth, WA, Australia. He was a Pao Yue Kong Chair Professor with Zhejiang University, Hangzhou, China, a Professor and the Chair of Electrical Engineering with the City University of London, and a University Distinguished Professor with the Guangdong University of Technology, Guangzhou, China. His current research interests include smart cities and smart grids.

Dr. Lai was the recipient of the IEEE Third Millennium Medal, the IEEE Power and Energy Society (IEEE/PES) UKRI Power Chapter Outstanding Engineer Award in 2000, the IEEE/PES Energy Development and Power Generation Committee Prize Paper in 2006 and 2009, the IEEE Systems, Man, and Cybernetics Society Outstanding Contribution Award in 2013 and 2014, the Most Active Technical Committee Award in 2016, and the Best Paper Award in the IEEE International Smart Cities Conference in 2020 to his research team. He is an Associate Editor for IEEE TRANSACTIONS ON SYSTEMS, MAN, AND CYBERNETICS: SYSTEMS, Editor-in-Chief of IEEE SMART CITIES NEWSLETTER, a Member of the IEEE SMART CITIES STEERING COMMITTEE, and the Chair of IEEE SMC SOCIETY STANDARDS COMMITTEE. He was a Member of the IEEE SMART GRID STEERING COMMITTEE, the Director of Research and Development Center, State Grid Energy Research Institute, China, the Vice President for Membership and Student Activities of IEEE SMC Society, and a Fellow Committee Evaluator and a Distinguished Lecturer of the IEEE Industrial Electronics Society. He is an IET Fellow.